

Article

In-Situ Sludge Reduction in Membrane-Controlled Anoxic-Oxic-Anoxic Bioreactor: Performance and Mechanism

Chengyue Li ^{1,2,3,†}, Tahir Maqbool ^{1,2,3,†}, Hongyu Kang ^{1,2,3} and Zhenghua Zhang ^{1,2,3,*} 

¹ Institute of Environmental Engineering & Nano-Technology, Tsinghua Shenzhen International Graduate School, Tsinghua University, Shenzhen 518055, China; li-cy19@mails.tsinghua.edu.cn (C.L.); tahir.maqbool702@gmail.com (T.M.); khy20@mails.tsinghua.edu.cn (H.K.)

² Guangdong Provincial Engineering Research Centre for Urban Water Recycling and Environmental Safety, Tsinghua Shenzhen International Graduate School, Tsinghua University, Shenzhen 518055, China

³ School of Environment, Tsinghua University, Beijing 100084, China

* Correspondence: zhenghua.zhang@sz.tsinghua.edu.cn

† These authors contributed equally to this work.

Abstract: Conventional and advanced biological wastewater treatment systems generate excess sludge, which causes socio-economic and environmental issues. This study investigated the performance of membrane-controlled anoxic-oxic-anoxic (AOA) bioreactors for in-situ sludge reduction compared to the conventional anoxic-oxic-oxic membrane bioreactor (MBR_{control}). The membrane units in the AOA bioreactors were operated as anoxic reactors at lower sludge recirculation rates to achieve hydrolysis of extracellular polymeric substances (EPS) and extensive endogenous respiration. Compared to MBR_{control}, the AOA bioreactors operated with 90%, and 80% recirculation rates reduced the sludge growth up to 19% and 30%, respectively. Protein-like components were enriched in AOA bioreactors while fulvic-like components were dominant in MBR_{control}. The growth of *Dechloromonas* and *Zoogloea* genera was promoted in AOA bioreactors and thus sludge reduction was facilitated. Metagenomics analysis uncovered that AOA bioreactors exhibited higher proportions of key genes encoding enzymes involved in the glycolysis and denitrification processes, which contributed to the utilization of carbon sources and nitrogen consumption and thus sludge reduction.

Keywords: membrane bioreactor; sludge reduction; endogenous respiration; denitrification; metabolic pathways



Citation: Li, C.; Maqbool, T.; Kang, H.; Zhang, Z. In-Situ Sludge Reduction in Membrane-Controlled Anoxic-Oxic-Anoxic Bioreactor: Performance and Mechanism. *Membranes* **2022**, *12*, 659. <https://doi.org/10.3390/membranes12070659>

Academic Editor: Anja Drews

Received: 2 June 2022

Accepted: 23 June 2022

Published: 27 June 2022

Publisher's Note: MDPI stays neutral with regard to jurisdictional claims in published maps and institutional affiliations.



Copyright: © 2022 by the authors. Licensee MDPI, Basel, Switzerland. This article is an open access article distributed under the terms and conditions of the Creative Commons Attribution (CC BY) license (<https://creativecommons.org/licenses/by/4.0/>).

1. Introduction

The activated sludge process is well-adapted for domestic and industrial wastewater treatment [1–3]. The extensive biomass generation in such retention systems also remains a tricky problem from a socio-economic and sustainable environment perspective since the excess sludge contains various hazardous substances and the management cost is considerably high [4–6]. Therefore, more financial investment and consideration are required for sludge handling and disposal [7]. In recent years, the stringent environmental legislation (GB18918-2002) and the 12th Five-Year Plan of China, which began in 2011, have already put forward new policies on excess sludge disposal and management [8].

Nowadays, researchers are working on multiple end-of-pipe solutions for the cost-effective mitigation of excess sludge [1,8]. In this regard, in-situ sludge reduction in biological wastewater treatment systems is an emerging concept in tackling the issue. In the last two decades, several studies have reported the effectiveness of the oxic-settling anoxic (OSA) process to reduce biomass by minimizing bacterial growth. The additional anoxic/anaerobic unit in the OSA process accelerates particular microbial functions, limiting bacterial growth [9]. Although trials are only found at the lab-scale levels, the OSA (as a side-stream reactor) concept has also been extended to MBR. For this purpose, biomass from the membrane tank is passed through an additional anoxic/anaerobic retention reactor [10].

However, additional installation in existing MBRs would raise technical and economic issues. For example, Wang et al. [11] installed an additional anaerobic side-stream reactor (ASSR) with a working volume of 50 L to the MBR, increasing a total volume up to 75% and achieving a sludge reduction of 21.7%. As such, there is a compelling need for a configuration of MBR, which could promote the in-situ sludge reduction while retaining the efficiency of the system. Furthermore, the underlying mechanisms for sludge reduction are complex and still unclear. In general, researchers have proposed that the cryptic growth, maintenance metabolism, destruction of EPS, hydrolysis of particulate organic matters (POMs), predation, endogenous metabolism and uncoupling metabolism are the common causes for sludge reduction. These phenomena were controlled by regulating the slow-growing bacteria, predators, hydrolytic and fermentative microorganisms [12–15]. Although much attention has been paid on the effect of different operational parameters on sludge minimization, nutrient removal and the dynamics of the microbial community composition in MBR-SSR systems (SSR: side-stream reactor), few studies elucidate the details from the perspective of metabolic pathways in the sludge reduction process. Recently, Zhao et al. [16] investigated the nitrogen metabolic pathways and key functional genes in the MBR-APSSR system (APSSR: ASSR packed with carriers) by metagenomics analysis and found the correlation between nitrogen consumption and sludge reduction. However, no study discusses the carbon metabolism in such systems. Exploring the carbon and nitrogen metabolic pathways could help the understanding of the sludge reduction mechanism.

Based on the abovementioned knowledge gaps, this study evaluated the membrane-controlled anoxic-oxic-anoxic (AOA) bioreactors that performed in-situ sludge reduction without chemicals addition or a side-stream reactor. The specific objectives of the study are: (i) operating the AOA bioreactors at lower sludge interchange rates with the purpose of severe endogenous respiration conditions in the membrane tank (M-tank), (ii) comparing the impact of different sludge interchange rates in different AOA bioreactors on biomass yield, detailed characterization of dissolved organic matter (DOM), (iii) exploring the mechanisms of sludge reduction by 16S rRNA amplicon sequencing and metagenomics.

2. Materials and Method

2.1. Experimental Setups

As shown in Figure 1, two membrane-controlled anoxic-oxic-anoxic (AOA) bioreactors with a working volume of 7.4 L each were operated in parallel. A conventional anoxic-oxic-oxic MBR_{control} having a scheme of an anoxic unit (2.0 L) (DO < 0.5 mg/L), an oxic unit (3.2 L) (DO of 1.5–2.5 mg/L), and a membrane tank as an oxic chamber (DO of 1.5–2.5 mg/L) with a volume of 2.2 L was considered as control, and mixed liquor shifting from anoxic to oxic units in MBR_{control} was controlled by gravity flow mixing (Figure 1). In membrane-controlled AOA bioreactors, membrane tanks (2.2 L) were operated in anoxic conditions (DO < 0.5 mg/L) following the typical pre-anoxic (2.0 L) and oxic units (3.2 L). In AOA bioreactors, mixed liquor shifting was controlled using peristaltic pumps from anoxic to oxic to M-tank rather than the gravity flow mixing. Lower sludge recirculation (<100%) from the M-tank to the anoxic unit allowed the higher concentration of the biomass in the M-tank than the respective anoxic and oxic units in AOA bioreactors.

One of the AOA bioreactors was operated with a 90% recirculation rate (AOA₉₀) and the other with 80% (AOA₈₀) (Figure 1). These recirculation rates were calculated based on permeate flux (5 LMH). AOA₉₀ and AOA₈₀ were operated with the respective recirculation rates of 90% and 80% for 23 h every day; however, for one hour of 24 h every day, the recirculation rates of these lines were increased to 1800% and 1600% for AOA₉₀ and AOA₈₀, respectively. In this way, famine/feast conditions were controlled in M-tanks of AOA bioreactors. After 23 h of operation each day, the mixed liquor suspended solid (MLSS) concentration was lower in anoxic and oxic units compared to the M-tanks of AOA bioreactors. The recirculation from the oxic to the anoxic unit was kept the same, i.e., 200%, in all bioreactors (MBR_{control}, AOA₉₀ and AOA₈₀). The same synthetic wastewater was used for all MBRs, and the detailed composition is presented in the Supporting Information

(Table S1). The synthetic wastewater containing glucose, ammonium chloride (NH_4Cl), sodium nitrate (NaNO_3) and potassium dihydrogen phosphate (KH_2PO_4) was used as the major source of carbon (DOC: 399 mg/L), nitrogen (TN: 40 mg/L) and phosphorous (TP: 6 mg/L), respectively. Micro-nutrients (i.e., MgSO_4 and FeCl_3) were also added in trace amounts. The pH of reactors was maintained at around 7.0 by adding NaHCO_3 in the feed. The operation comprised two phases, i.e., acclimatization phase (112 days) and stable phase (90 days), which were determined based on MLSS.

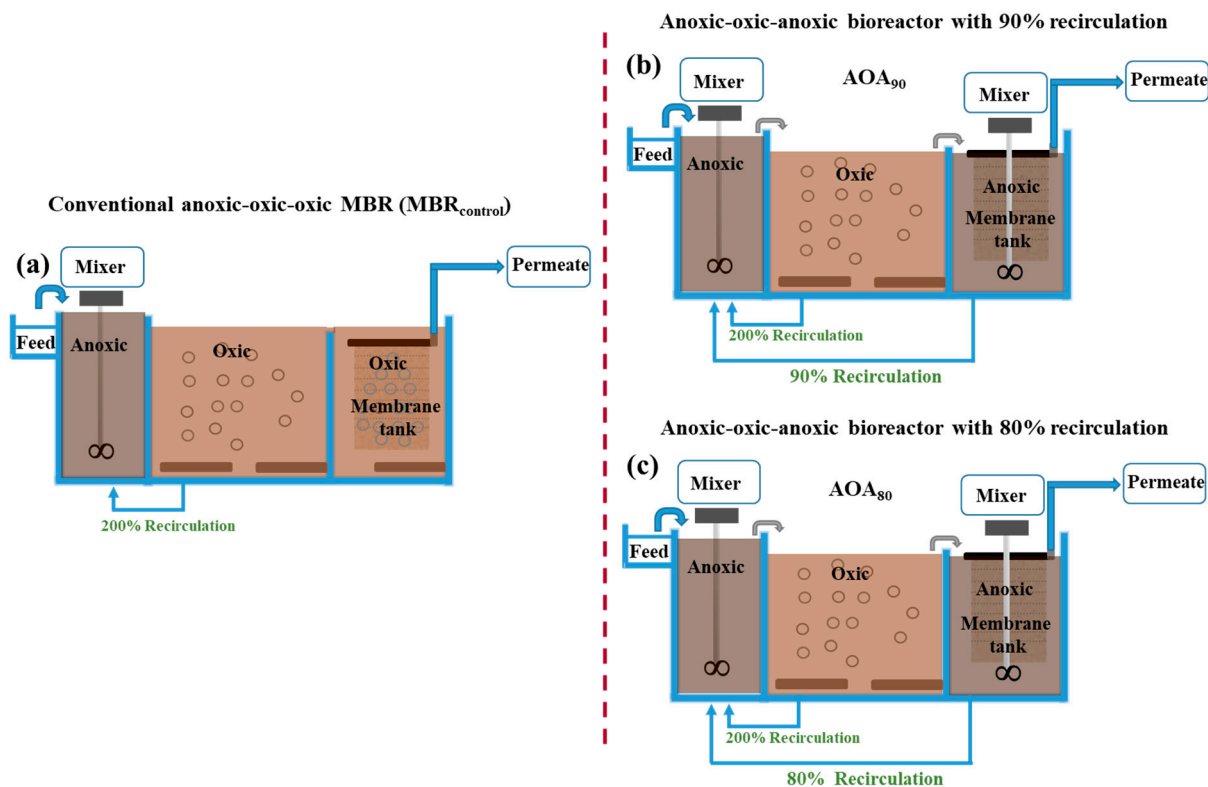


Figure 1. Configuration of conventional anoxic-oxic-oxic MBR ($\text{MBR}_{\text{control}}$) (a) and membrane controlled anoxic-oxic-anoxic bioreactors with 90% (AOA_{90}) (b) and 80% (AOA_{80}) (c) recirculation.

Flat sheet ceramic membrane modules were purchased from Meidensha, Japan, with a nominal pore size of $0.1 \mu\text{m}$ and an effective area of 0.0425 m^2 , and were used in all bioreactors. The operating parameters such as sludge retention time (SRT), hydraulic retention time (HRT) and flux of AOA bioreactors and $\text{MBR}_{\text{control}}$ were 80 days, 34 h, and 5 LMH, respectively. The maximum allowable transmembrane pressure (TMP) was designed to be 30 kPa, after which membrane modules were both physically and chemically cleaned.

2.2. Extraction and Characterization of EPS and SMP

The supernatant containing soluble microbial product (SMP) was separated from sludge flocs by centrifuging the mixed liquor at 4000 rpm and $4 \text{ }^\circ\text{C}$. EPS was extracted by adopting the so-called heating method described in Xiao et al. [17], with some modifications. The flocs were re-suspended in a 0.05% NaCl solution, and heated at $70 \text{ }^\circ\text{C}$ in a water bath for 30 min, and centrifuged at 4000 rpm to collect the bound EPS. All these EPS were filtered through a $0.45 \mu\text{m}$ membrane filter and stored at $-10 \text{ }^\circ\text{C}$ for further analytical measurements. The protein and polysaccharide contents in EPS and SMP were characterized using Lowry and phenol/ H_2SO_4 methods, respectively [18,19].

2.3. Analytical Characterization

The pH of mixed liquor was regularly monitored using a desktop pH meter (Thermo, Waltham, MA, USA). Dissolved organic carbon (DOC) and total dissolved nitrogen (TN)

were measured using the TOC-V analyzer (Shimadzu, Kyoto, Japan). The nutrients, including ammonium (NH_4^+), nitrate (NO_3^-) and total phosphate (TP) concentrations, were determined using a colorimetric method as given in the Standard Examination Methods for Drinking Water—Nonmetal Parameters, China (GB/T 5750.5-2006). The mixed liquor suspended solids (MLSS) were measured using APHA standard methods [20].

The significant difference was analyzed with the Origin software using one-way ANOVA test. Principle component analysis (PCA) was also implemented by the Origin software.

2.4. PARAFAC Modeling

Fluorescence spectra in the form of a three-dimensional excitation-emission matrix (EEM) were collected from a fluorescence spectrometer (F-7000 Hitachi, Tokyo, Japan). The fluorometer was operated with the following adjusted parameters: excitation (Ex) and emission (Em) wavelength ranges were set to 220–500 nm and 240–550 nm with the incremental step of 5 nm and 1 nm, respectively. The scan speed was 12,000 nm/min, and the slit size (Ex/Em) was fixed at 10 nm. The EEMs of blanks (Milli-Q) were also measured regularly and subtracted from the EEMs of samples. A dataset consisting of 326 EEMs of EPS and SMP from three MBRs was used for PARAFAC modeling. A free toolbox, DOMFlour, was used in Matlab (MathWorks Inc., Natick, Massachusetts, USA), and a tutorial by Stedmon and Bro (2008) was followed. Detailed steps could be found elsewhere [21,22].

2.5. 16S rRNA Amplicon Sequencing and Metagenomics Analysis

The sludge samples under steady state at different stages of the experiment, i.e., 0, 45th, and 90th day of operation, were collected from each reactor for microbial analysis. The sludge samples were analyzed by MAGIGENE (Guangzhou, China) for high-throughput sequencing. Deoxyribonucleic acid (DNA) was extracted using the Power Soil DNA Isolation Kit (MOBIO, San Diego, CA, USA). The amplification of the V4-V5 regions of the extracted DNA was obtained using the specific 16S rRNA (515F/907R) as a primer by polymerase chain reaction (PCR). The PCR procedures were conducted using the BioRad S1000 (Bio-Rad Laboratory, Hercules, CA, USA) following the protocol developed by the manufacturer. The purification of the PCR products and the quality control, and construction of sequencing library were obtained by following a previous study of Renetal [23]. The library sequencing was performed using the Illumina Nova Seq 6000 platform and 250 bp paired-end reads were obtained. Finally, a range of detailed DNA sequence analyses were performed in accordance with Ren et al. [23].

The sludge samples in the M-tank of three reactors were collected for metagenomics analysis. In this case, a total of nine samples were obtained for DNA extraction, and the Illumina Miseq 2500 platform was applied for metagenomic sequencing analysis after library preparation. The glucose and nitrogen metabolism pathway maps were determined from the Kyoto Encyclopedia of Genes and Genomes (KEGG) database, and the relative abundances of different functional categories were calculated based on gene annotation results from each database.

3. Results and Discussion

3.1. Basic Water Quality Parameters

The temporal and average of the long-term system performances of bioreactors in terms of DOC and nutrient removals (TN and TP) are presented in Figure S1 and Table S2. The results are only presented for the stable phase. The results showed effective removal of organic substrates and nutrients (TN and TP) in all three bioreactors. The effluents obtained from these systems had reasonable qualities for discharge [24]. The extensive removal (>99%) of organic substrates could be ascribed to the long designed SRT (i.e., 80 days). Previous studies also achieved refined quality of effluent at such prolonged retention [25,26]. It deduced from the results that the performance of AOA bioreactors remained intact compared to $\text{MBR}_{\text{control}}$ in removing organics and nutrients. Remarkable

TN removal in three bioreactors was achieved with the effluent concentration of 2.43 ± 1.76 , 2.19 ± 1.23 and 1.77 ± 1.55 mg/L in MBR_{control}, AOA₉₀ and AOA₈₀, respectively. Although the difference among the TN concentration in effluents was not statistically significant, the AOA bioreactors seemed to be more efficient than MBR_{control}. On the other hand, the TP removal was slightly lower in effluents obtained from AOA bioreactors with an average of 0.62 ± 0.46 and 0.65 ± 0.25 mg/L for AOA₉₀ and AOA₈₀, respectively.

The role of different treatment units (anoxic/oxic/M-tank) in removing TN (NH_4^+ and NO_3^-) species was also elucidated and presented in Figure S2 and Table S3. In MBR_{control}, a gradual decrease in NH_4^+ concentration was recorded from anoxic to oxic to M-tank, highlighting the direct role of the oxic condition in removing nutrients. At the same time, NO_3^- was increased from an anoxic to an oxic unit in MBR_{control}, presenting the transformation of NH_4^+ ($p < 0.05$). In AOA bioreactors, the anoxic unit showed the highest NH_4^+ concentration, 6.71 ± 2.18 and 3.23 ± 2.87 mg/L, and the lowest NH_4^+ concentration was found in the oxic unit, 0.47 ± 0.63 and 0.25 ± 0.31 mg/L, in AOA₉₀ and AOA₈₀, respectively. The extended anoxic condition in AOA bioreactors was found helpful in removing NO_3^- with prolonged denitrification. In general, results proved the efficient working of membrane-controlled AOA bioreactors, which did not halt any general phenomenon in a typical MBR but provided extra removal of NO_3^- . The additional removals are also justified based on previous studies related to OSA processes or coupling side-stream reactors to MBR and the sulfidogenic OSA processes. For instance, Zhou et al. [27] also reported the enhanced removal of TN in OSA compared to the conventional activated sludge process; similar to the current study, a slight increase in NH_4^+ was also found due to hydrolysis. In another study, marginally improved nutrient removal was reported due to a coupled SSR [28]. Coupling the SSR to MBR also caused a slight increase in NH_4^+ concentration but reduced TN in the effluent than the control MBR [10]. This study did not use any additional reactor; instead, it managed the feast/famine conditions in the M-tank and promoted in-situ sludge hydrolysis and reduction compared to all these reports.

3.2. Sludge Reduction

The changes in the averaged MLSS concentration during unstable and stable phases of operation are presented in Figure 2a. A relatively consistent averaged MLSS was obtained after more than 100 days of operation. The averaged MLSS concentration in the stable phase was found to be 4.40 ± 0.26 , 3.55 ± 0.21 , and 3.17 ± 0.23 g/L for MBR_{control}, AOA₉₀, and AOA₈₀, respectively. The MLSS concentration in different tanks of MBR_{control}, AOA₉₀, and AOA₈₀ was shown in Figure S3. These results presented up to a 20% and 30% reduction in MLSS with recirculation rates of 90% and 80% in AOA bioreactors, respectively.

However, the calculations of the observed yield were based on the MLSS obtained during the stable phase of operation only. The observed yield coefficient (Y_{obs}) was calculated by the slope of the increase in cumulative sludge generated (g MLSS) and cumulative consumed substrate (g DOC), as presented in Figure 2b. This approach of calculating yield was adopted in several previous studies related to sludge reduction in activated sludge processes [4,28]. The factors like SRT were also considered in such calculation, which was constant for all bioreactors. The cumulative sludge generated was based on the average of MLSS in anoxic, oxic and M-tanks. The results showed that the Y_{obs} of MBR_{control} was 0.31 gMLSS/g DOC, which was relatively lower than the previous studies, with the usual value of around ~ 0.4 gMLSS/g COD [29,30]. Longer SRT (i.e., 80 days) could be ascribed to such lower yield in MBR_{control}, promoting endogenous respiration for cell maintenance and leading to cell lysis and decay [31,32]. Several previous studies compared the impact of different SRTs on sludge yield in MBR and other biological systems; lower yield with cryptic growth and lysis has been reported at prolonged retention conditions [33,34].

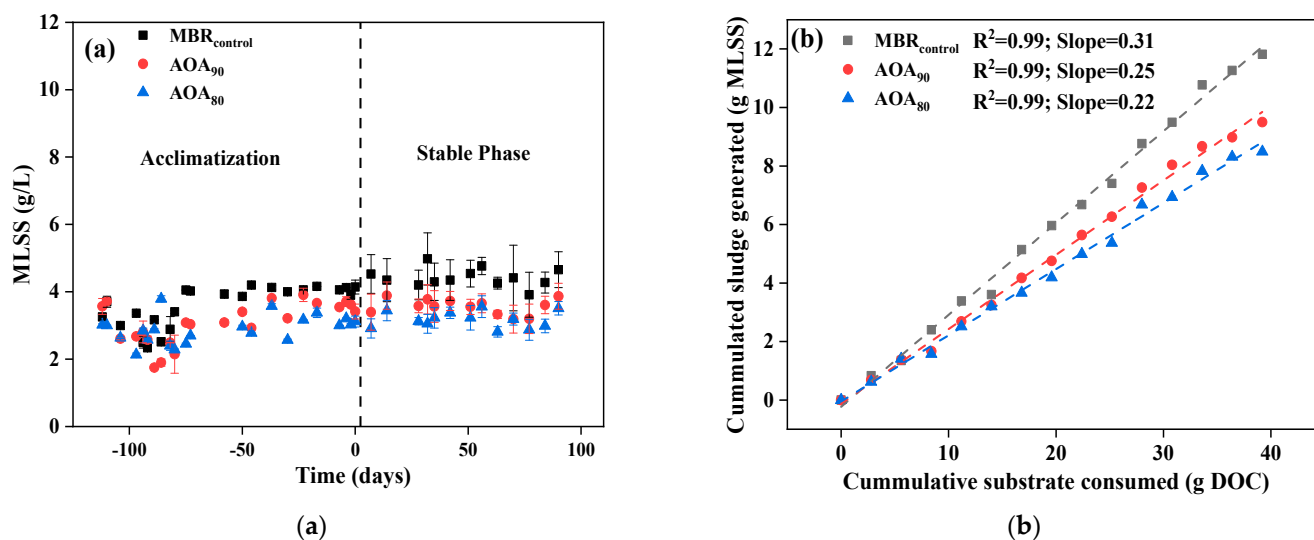


Figure 2. (a) The change in the averaged MLSS concentration between acclimatization and stable operation phases in MBR_{control}, AOA₉₀ and AOA₈₀, (b) The observed sludge yield (Y_{obs}) in MBR_{control}, AOA₉₀ and AOA₈₀.

Compared to MBR_{control} ($Y_{obs} = 0.31$), the Y_{obs} for AOA₉₀ and AOA₈₀ were found to be 0.25 and 0.22 gMLSS/gDOC, respectively. These results infer that the operational scheme of AOA bioreactors successfully reduced sludge biomass up to 19.35% and 29.03% at recirculation rates of 90% and 80%, respectively. Such a reduction in biomass yield indicates the role of multiple factors, including cell lysis, hydrolysis of particulate to DOM, and cryptic growth in the M-tank of the AOA bioreactors. The gradual concentrating biomass in M-tank with lower recirculation rates was found effective in controlling the sludge yield with equivalent or better performance in removing pollutants. The higher MLSS in famine conditions instigated the phenomenon of self and in-situ reduction of biomass in the anoxic condition in M-tank.

3.3. Dynamics of EPS and SMP in AOA Bioreactors

The AOA configurations brought a substantial reduction in sludge growth, and such endogenous conditions also promoted the hydrolysis of EPS, as presented in Figure 3. In MBR_{control}, the total EPS in terms of average DOC/g MLSS was found in a decreased order from anoxic to oxic to M-tank; however, the difference among the units was statistically insignificant ($p > 0.05$). The AOA bioreactors showed contrasting results for corresponding units in MBR_{control} ($p < 0.05$). The AOA₉₀ showed an increase in EPS concentration than MBR_{control}; however, EPS in AOA₈₀ was noticeably lower in each reactor than MBR_{control} and AOA₉₀. The higher EPS production in the anoxic and oxic units of AOA₉₀ could be due to pseudo-endogenous respiration, which probably suppressed the microbial functioning in the anoxic M-tank. Upon return to the pre-anoxic unit, microorganisms regained activity in response to feast conditions there. It is worth mentioning that F/M in both membrane-controlled AOA bioreactors shifted from the start of 24 h to the end. At 0 h, the F/M was highest in anoxic and oxic units and lowest in the M-tank and was vice-versa at the 24th hour. In AOA₈₀, extreme biomass retention in the M-tank possibly caused hydrolysis of bound EPS, which inhibited the microbial functioning extensively and promoted sludge digestion. The extreme digestion seized the microbial activity for an extended period, which was even not recovered while recirculating to an anoxic chamber and followed by an oxic chamber.

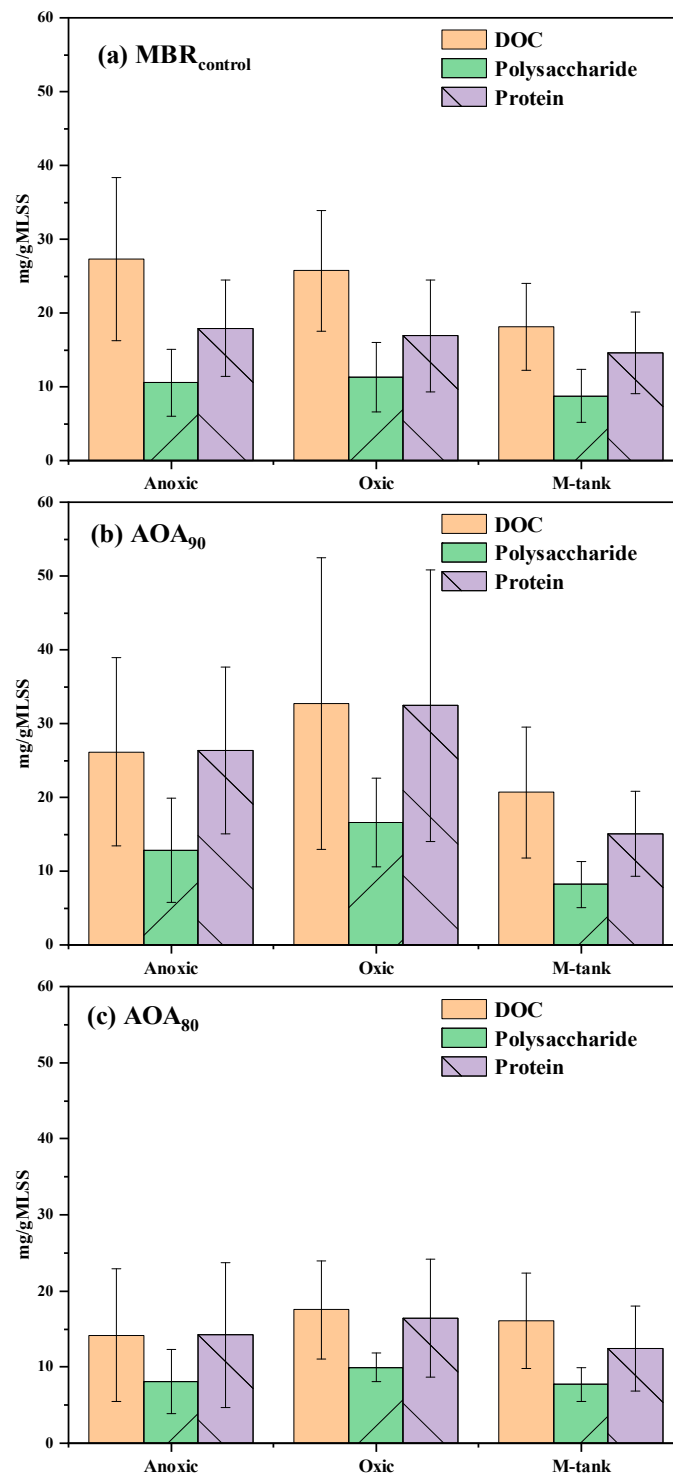


Figure 3. The average of total EPS in terms of DOC, polysaccharides, and protein in different units of bioreactors ($n = 14$).

The EPS contents, protein, and polysaccharides were found abundant in the anoxic and oxic units of AOA₉₀ compared to AOA₈₀ and MBR_{control} ($p < 0.05$) (Figure 3). The average polysaccharide vs. protein in M-tanks of MBR_{control}, AOA₉₀, and AOA₈₀ was recorded to be 8.75 ± 3.58 vs. 14.58 ± 5.48 , 8.2 ± 3.11 vs. 15.04 ± 5.74 , and 7.71 ± 2.18 vs. 12.43 ± 5.64 mg/gMLSS, respectively. The results presented an insignificant difference in the average concentration of EPS in the M-tanks of all the bioreactors. It is deduced from the results that the configuration of the AOA bioreactor showed the capability to reduce

biomass while keeping EPS at a matching level to MBR_{control}. The changes in SMP in AOA bioreactors were also measured and presented in Figure S4. The SMP in the anoxic and oxic units in AOA₉₀ and AOA₈₀ could interfere with the supernatant DOC with possible low degradation; therefore, only changes in polysaccharide and protein in SMP were elucidated. The polysaccharide concentration in the M-tank of MBR_{control}, AOA₉₀, and AOA₈₀ was 1.11 ± 0.60 , 1.80 ± 1.49 and 5.46 ± 4.84 mg/L, respectively, indicating the release of intracellular polysaccharide in AOA bioreactors. The protein concentration in the M-tank of MBR_{control}, AOA₉₀, and AOA₈₀ was 2.97 ± 2.67 , 4.80 ± 2.76 and 3.18 ± 2.18 mg/L, respectively. The relatively higher protein concentration in AOA bioreactors was possibly due to cell lysis and hydrolysis that occurred during in-situ sludge reduction. The release of proteinous compounds during digestion or sludge reduction has been abundantly reported in previous studies related to anaerobic digestion and OSA processes [35]. In addition, studies have demonstrated that in anoxic conditions, SMP could be re-utilized as electron donors by bacteria for denitrification [36,37]. Considering the higher TN removal efficiency in the AOA₈₀ bioreactor, it could be speculated that the generated protein was quickly metabolized by the denitrifying bacteria in the AOA₈₀ bioreactor. As such, the protein concentration in the M-tank followed the order: AOA₉₀ > AOA₈₀ > MBR_{control}.

The DOM composition in EPS and SMP could help understand the phenomenon behind the sludge reduction. Several indicators are suggested in previous studies for separating the different respiration conditions, hydrolysis, and cell lysis [38]. As such, the DOM composition and concentration changes were explored to better understand the mechanism of in-situ sludge reduction.

The maps of the three components with their peak positions of EEM-PARAFAC modeling are presented in Figure S5. One component (C1) showed a resemblance to the protein-like fluorescence, with its features matching to tryptophan-like. The other two components, C2 and C3, represent the fulvic-like and humic-like fluorescence, respectively [39–44]. The distribution of fluorescence components in the SMP and EPS from different units of bioreactors is presented in Figure 4. The fulvic-like C2 was found abundant in SMP of MBR_{control}, which could be generated by the microbial degradation of organics with abundant oxygen [45]. The total fluorescence intensity was found to decrease from anoxic to oxic to M-tank, and the average reduction was recorded to around 20%. These changes could be linked to the increasing performance along the treatment train as reflected by the basic water quality parameters, such as NH₄⁺ removal. In contrast, the protein-like component showed a higher share in SMP than fulvic-like components in AOA bioreactors. Moreover, changes in composition were noticeable among the different treatment units; the anoxic tank and M-tank showed similar composition. The SMP enriched with the protein-like component in the anoxic unit and M-tank indicated the cell lysis due to extensive biomass retention and the SMP composition was found similar ($p > 0.05$). However, a noticeable difference was recorded in total component intensity (R.U.) between the bioreactors. AOA₉₀ produced a relatively lower SMP concentration as fluorescent DOM (FDOM) than AOA₈₀. The average total component was higher in the anoxic tank and M-tank of AOA bioreactors than MBR_{control}. Cell lysis and hydrolysis during in-situ sludge reduction could be the causes of such change in FDOM. Similarly, adding a side-stream reactor to MBR was reported to cause the higher release of FDOM, and an anaerobic sludge digester also released SMP enriched with protein [30,46].

The EPS-related FDOM was measured in terms of R.U./g MLSS and is presented in Figure 4. In all units of bioreactors, protein was noted to be the leading component with a contribution of above 85%. A direct influence of the extra sludge in terms of decreased R.U./gMLSS in M-tanks of AOA₈₀ and AOA₉₀ was recorded. The decreased EPS in the M-tanks of AOA bioreactors indicated the consumption of polymeric substances attached to microorganisms and inside the microbial flocs. Oxic units in AOA₉₀ and AOA₈₀ showed higher FDOM up to 10.0 R.U./gMLSS and 5.0 R.U./gMLSS, respectively. Among the bioreactors, AOA₈₀ has the lowest R.U./gMLSS. It infers that extensive sludge reduction substantially controlled the yield of biomass and suppressed the EPS.

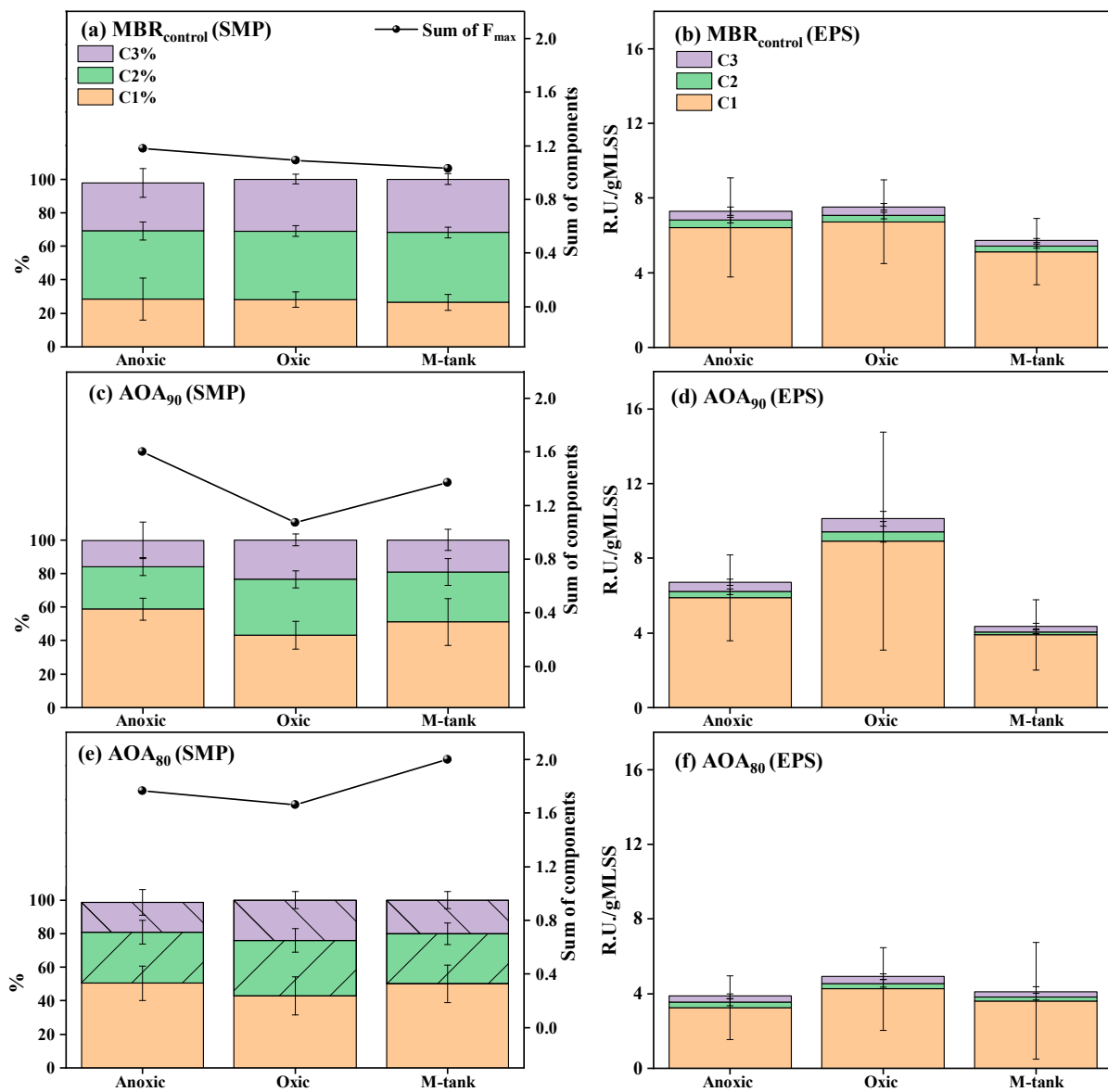


Figure 4. The average distribution of EEM-PARAFAC components and sum of F_{max} (C1 + C2 + C3) in SMP and EPS of different units in (a,b) $MBR_{control}$, (c,d) AOA_{90} , and (e,f) AOA_{80} ($n = 14$).

3.4. Microbial Community

The variation in sludge recirculation ratio altered the F/M as well as the microorganisms in the bioreactors. The evolution of the microbial community was monitored and presented in Table S4 and Figure 5a,b. In $MBR_{control}$, the Simpson index first increased and then decreased, with the highest value in the mid-term operation period. In AOA_{90} , an opposite trend for microbial enrichment was observed compared to $MBR_{control}$. However, the Simpson index in AOA_{80} increased with the operation time, indicating the decreased microbial diversity. The substrate-limited environment in the M-tank caused sludge hydrolysis and thus possibly decreased the microbial diversity. Meanwhile, the richness of the microbial species decreased with time in all three bioreactors, and AOA_{80} had the lowest richness. The 80% recirculation ratio promoted the starvation conditions, which led to the biomass decay in AOA_{80} . The varying recirculation rate of sludge from the membrane tank to the pre-anoxic tank would affect microbial community relationships to carry out in-situ sludge reduction in the bioreactors [10], which will be discussed in the following section.

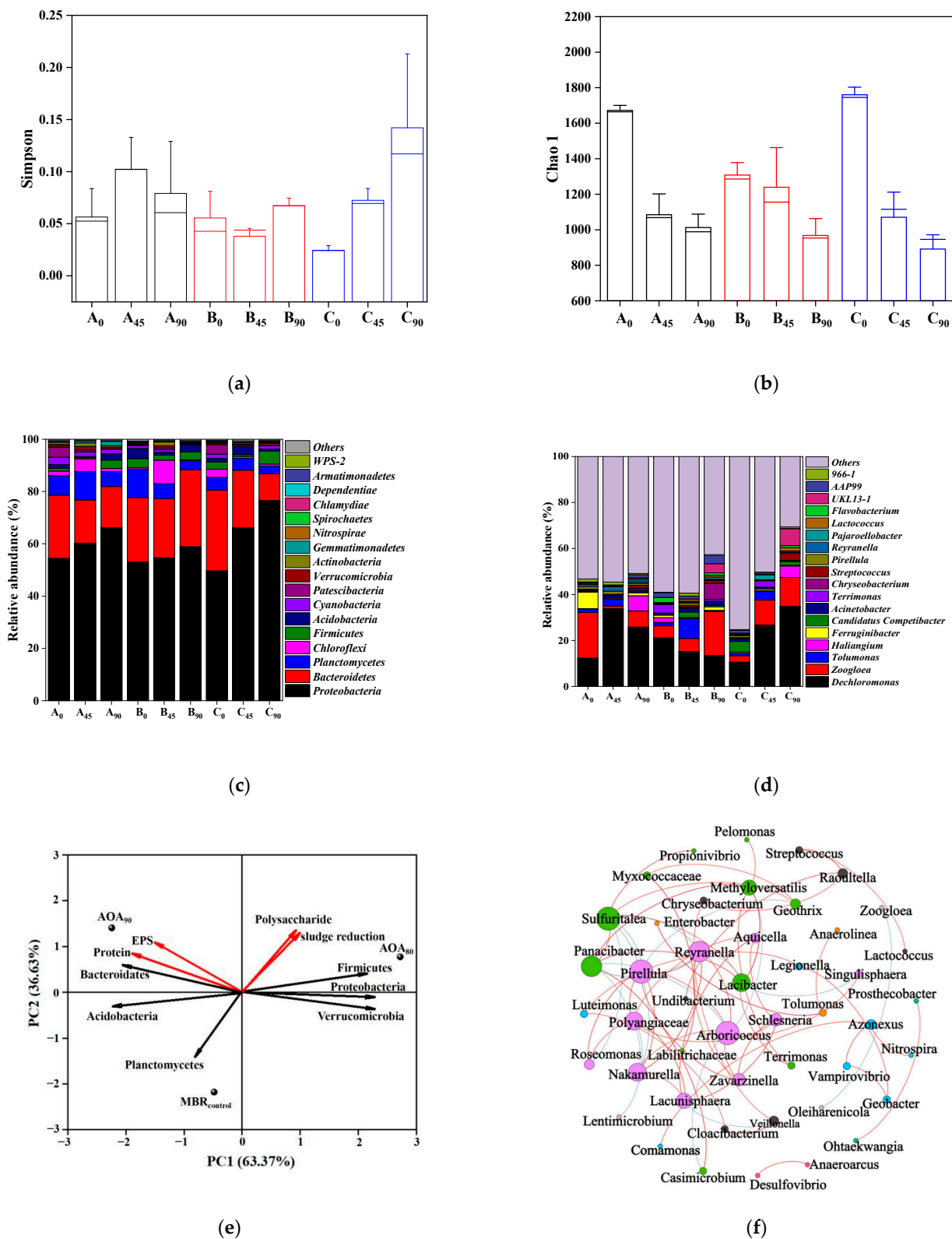


Figure 5. The Simpson index (a), Chao 1 index (b), relative abundance of dominant species at the phylum level (c) and genus level (d), PCA between bacteria community at the phylum level and sludge reduction (e) and co-occurrence network (f). (A, B, and C represent MBR_{control}, AOA₉₀ and AOA₈₀, respectively, and the subscript of A, B, and C means the sampling time).

The microbial composition was classified at the phylum level, as presented in Figure 5c. *Proteobacteria*, *Bacteroidetes*, *Firmicutes* and *Planctomycetes* were the major phyla throughout the sludge reduction process. In all the bioreactors, the relative abundance of *Proteobacteria* increased with the operation time, and AOA₈₀ had the highest abundance at the 90th day of operation. *Proteobacteria* was known as the dominant hydrolytic and acidogenic bacteria with the potential for polysaccharide degradation [47]. *Bacteroidetes* played a strong role in large molecular organic matter degradation, i.e., proteins and polysaccharides [48]. The relative abundance of *Bacteroidetes* in AOA₉₀ increased with the operation time and became the highest among three bioreactors. *Firmicutes* was responsible for anoxic hydrolysis and acidification [49], and was beneficial for organic degradation [50]. The relative abundance of *Firmicutes* in AOA₈₀ was the highest than in other bioreactors at the 90th day of operation, in agreement with its best sludge reduction performance (Figure 2).

Further analysis of microbial community at the genus level was also conducted (Figure 5d). *Dechloromonas* and *Zoogloea* were the dominant genera of three bioreactors. *Dechloromonas*, the slow-growing bacteria with the function of denitrification [46], was the most abundant genus in AOA₈₀ (34.76% at the 90th day of operation). *Zoogloea* was known as the denitrifying bacteria [23] and could facilitate the removal of organic compounds [51]. The relative abundance of *Zoogloea* in AOA₉₀ was the highest among three bioreactors at the 90th day of operation. *Chryseobacterium* with the highest richness in AOA₉₀ would also induce EPS degradation due to its good proteolytic ability [52]; therefore, resulting in the cell lysis in AOA₉₀. These findings confirmed that the slow-growing and hydrolytic microorganisms played a critical role on the biomass reduction in AOA₉₀ and AOA₈₀ [53,54].

The correlation of the dominant phyla of microorganisms, sludge reduction, polysaccharide, protein and EPS was conducted via PCA analysis, as shown in Figure 5e. The respective contributions of the first and second axes to the total variance accounted for 63.37% and 36.63%, respectively. Obviously, the bacteria communities of MBR_{control}, AOA₉₀, and AOA₈₀ bioreactors were clustered separately, which indicated that the different sludge recirculation rates induced the evolution of the microbial communities. The positive correlation between sludge reduction and *Proteobacteria*, *Firmicutes* as well as *Verrucomicrobia* could be clearly identified, especially in AOA₈₀, while *Planctomycetes* had a totally negative correlation with sludge reduction in MBR_{control}. Meanwhile, *Firmicutes* and *Bacteroidetes*, phylum with the capability of organic degradation [48,50], were closely positive with polysaccharide removal in AOA₉₀ and protein removal in AOA₈₀, respectively.

The network analysis was conducted by Gephi (v 0.9.2) [55] to uncover the possible correlation (Pearson's correlation coefficient $\rho > 0.6$ and significance $p < 0.01$) between different genera in the bioreactors (Figure 5f). Different modules were distinguished by node colors, while node size was determined by the number of node connections. The orange and blue edges that connected two nodes were used to illustrate the positive and negative correlations [56]. Close positive relationships were found among dominant genera compared to negative interactions. The slow-growing bacteria *Sulfuritalea*, *Zavarinella* and *Azonexus* [26,54] exhibited a positive correlation with many other genera. *Sulfuritalea* was positively correlated with *Lacibacter*, *Pirellula* and *Reyranella*, which were able to hydrolyze organic compounds [57–59]. *Zavarinella* also showed a positive relationship with *Pirellula* and *Reyranella*. However, there was a negative correlation between *Roseomonas* and *Sulfuritalea*, which might be due to the competition or niche exclusion between these two species under limited substrate conditions [56]. *Azonexus*, *Comamons* and *Vampirovibrio* belonged to the same module, and *Azonexus* exhibited a positive relationship with *Comamons* and *Vampirovibrio*, the hydrolytic bacteria [60] and predatory bacteria [61], respectively. Moreover, the fermentative bacteria *Tolumonas* [62] correlated positively with *Anaerolinea*, one of the slow growing species [63]. Herein, positive networks were found between the slow-growing species, hydrolysis and fermentative bacteria, contributing to sludge reduction [56].

3.5. Metabolic Response Pathways

In spite of the change in the microbial community structure in three bioreactors, different sludge recirculation rates would also regulate the expression of functional genes. In this section, the carbon and nitrogen metabolic characteristics of three bioreactors were expounded.

3.5.1. Carbohydrate Metabolic Analysis and Functional Genes

Glycolysis is a significant part of carbohydrate metabolism, which converts glucose into pyruvate with energy liberation [48]. As presented in Figure 6, glucose was first converted into glucose-6P under the function of glucokinase (EC: 2.7.1.2) and polyphosphate glucokinase (EC: 2.7.1.63). The average relative abundance of glucokinase (polyphosphate glucokinase) was 0.0149% (0.0032%), 0.0165% (0.0023%), and 0.0186% (0.0027%) in MBR_{control}, AOA₉₀ and AOA₈₀, respectively, indicating that AOA₈₀ exhibited a higher proportion of key genes encoding enzymes in this step. Then, glucose-6-phosphate isomerase (EC: 5.3.1.9) catalyzed glucose-6P into fructose-6P and fructose-1, while 6P2 was formed with the function of 6-phosphofructokinase (EC: 2.7.1.11) followed by the triose phosphate isomerase reaction [48]. Later on, glyceraldehyde-3P was transformed into phosphoenolpyruvate after a series of reactions with the conversion between NAD⁺ and NADH along with ATP generation. Finally, pyruvate was produced with the catalysis of pyruvate kinase (EC: 2.7.1.40) and could be further metabolized into CO₂ [64]. The total relative abundance of genes encoding enzymes involved in the whole glycolysis process was 0.171%, 0.172%, and 0.184% in MBR_{control}, AOA₉₀ and AOA₈₀, respectively, suggesting that more energy would be provided in AOA₈₀ for microbial metabolism and organic degradation. During the glucose degradation process, the fructose-1, 6P2 and pyruvate production were the most important reactions, among which the former step was the rate-limiting procedure that controlled the whole glycolysis process [64]. The average proportions of genes encoding the two enzymes (EC: 2.7.1.11 vs. EC: 2.7.1.40) for the production of fructose-1, 6P2 and pyruvate in MBR_{control}, AOA₉₀ and AOA₈₀ were 0.0217% vs. 0.02%, 0.0244% vs. 0.022% and 0.0232% vs. 0.023%, respectively. This indicated that the glycolysis rate would be faster in AOA₉₀ and AOA₈₀ compared to MBR_{control}, implying enhanced microbial activity in AOA₉₀ and AOA₈₀ [65]. As such, the utilization rate of secondary substrates would be promoted in AOA₉₀ and AOA₈₀, which possibly resulted in improved sludge reduction efficiency.

3.5.2. Nitrogen Metabolic Analysis and Functional Genes

The nitrogen metabolic pathway and the comparative analysis of functional genes in three bioreactors were investigated as shown in Figure 7. The total relative abundance of genes encoding enzymes for the nitrification process was highest in MBR_{control}, followed by AOA₉₀ and AOA₈₀. The proportion of genes encoding the hydroxylamine dehydrogenase (EC: 1.7.2.6) reduced by 22.95% (AOA₉₀) and 35.86% (AOA₈₀) compared to MBR_{control}. Meanwhile, the contents of the genes encoding enzymes for ammoniation (EC: 1.14.99.39) and nitrite oxidoreductase (EC: 1.7.99.-) were highest in MBR_{control}. This was in good agreement with the lower concentration of NH₄⁺ in MBR_{control} as shown in Table S2. In contrast, the total relative abundance of genes encoding enzymes for the denitrification process was highest in AOA₈₀, followed by AOA₉₀ and MBR_{control}. The genes encoding the enzyme responsible for the reduction of nitrate to nitrite (EC: 1.9.6.1) and the genes encoding enzymes responsible for the reduction of nitrite and nitric oxide (EC: 1.7.2.1 and EC: 1.7.2.5) followed the order: AOA₈₀ > AOA₉₀ > MBR_{control}. Meanwhile, the average relative abundance of nitrous-oxide reductase (EC: 1.7.2.4) in AOA₉₀ was the highest (0.083%), followed by MBR_{control} and AOA₈₀ (0.071%). In addition, compared to MBR_{control}, the abundance of key genes related to denitrification, i.e., napAB, norBC and nosZ in AOA₉₀ and AOA₈₀ at the 90th day of operation increased by 44.88% vs. 139.30%, 33.08% vs. 162.77%, and 50.83% vs. 12.19%, respectively (Figure S6), indicating the enhanced denitrification process in AOA bioreactors. This was indeed the case and was in agreement

with the higher removal efficiency of TN in AOA bioreactors as shown in Table S2. The organics released from cell lysis and POM hydrolysis could be utilized as carbon sources for denitrification [66]. As such, more substances could be degraded in AOA bioreactors (especially in AOA₈₀), and thus resulting in the improved sludge reduction efficiency [67].

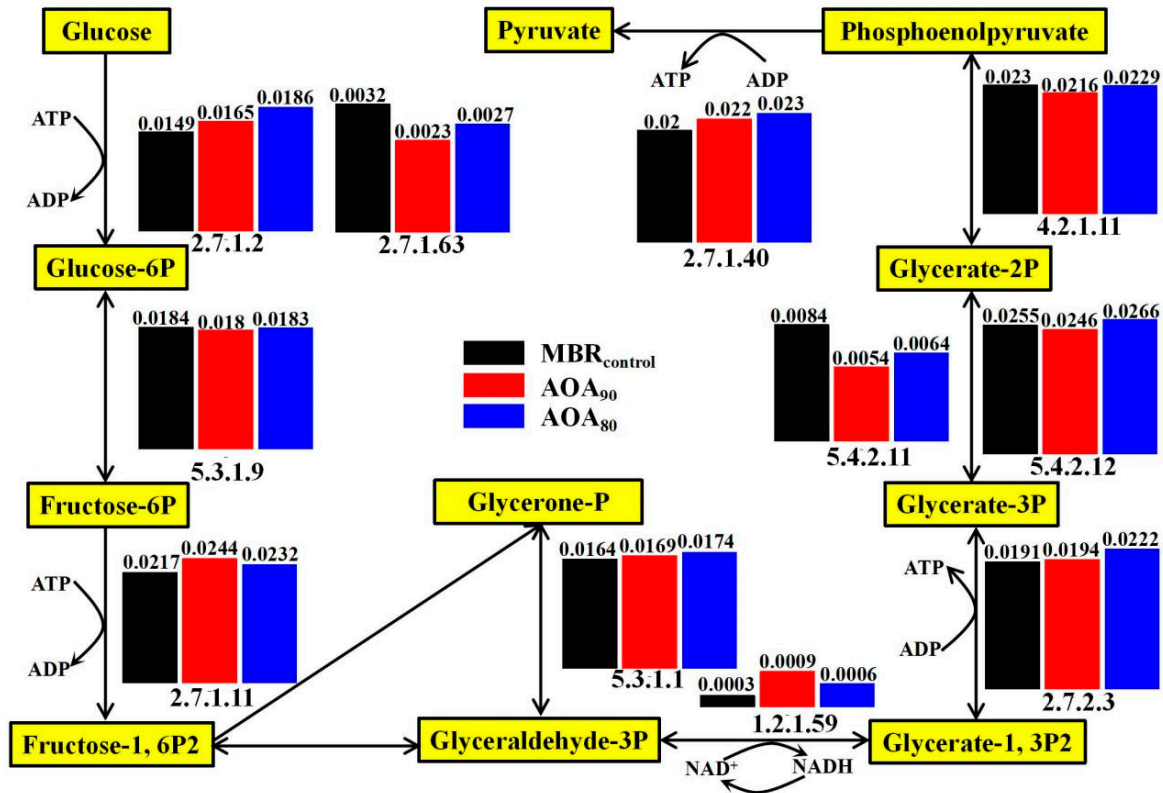


Figure 6. Diagram of glycolysis pathway and the average relative abundance of genes encoding enzymes (identified by their EC number) in MBR_{control}, AOA₉₀ and AOA₈₀.

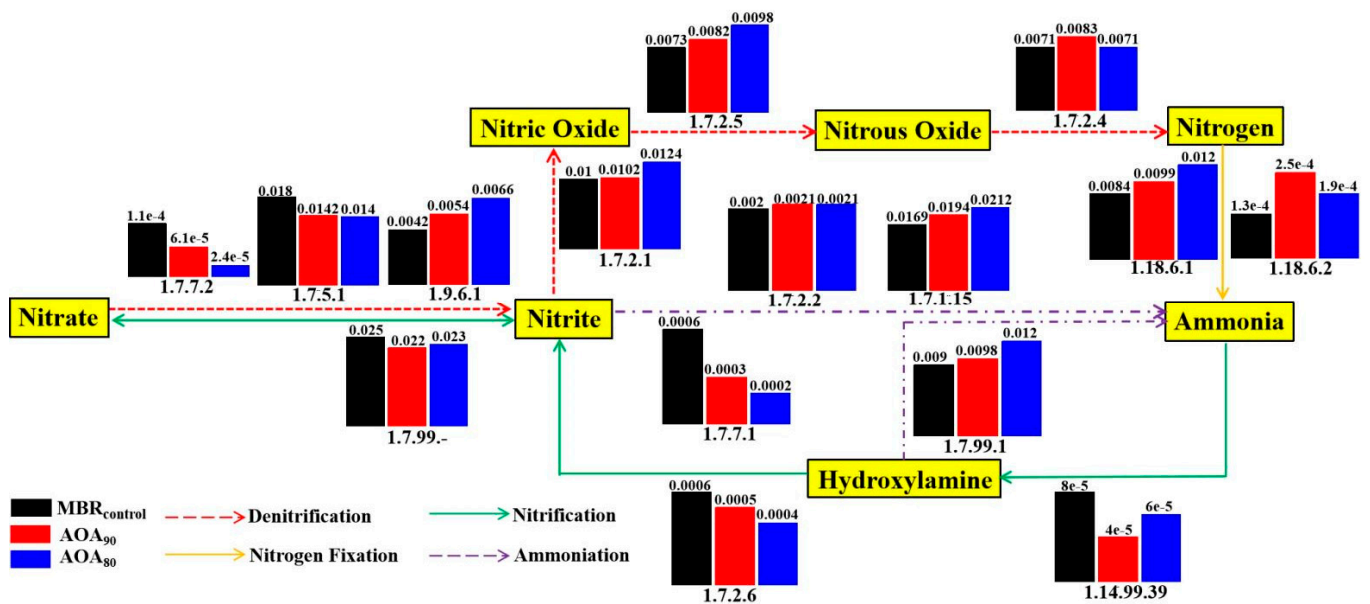


Figure 7. Diagram of nitrogen pathway and the average relative abundance of genes encoding enzymes (identified by their EC number) in MBR_{control}, AOA₉₀ and AOA₈₀.

4. Conclusions

The AOA bioreactors efficiently reduced sludge generation through promoting hydrolysis and endogenous respiration in the anoxic M-tank. Up to 30% sludge reduction with improved denitrification was achieved in the AOA₈₀ bioreactor. The decreased EPS in the anoxic M-tank of the AOA₈₀ bioreactor indicated the consumption of polymeric substances attached to microorganisms and inside the microbial flocs. The higher abundance of *Dechloromonas* and *Zooglea* in AOA bioreactors facilitated the sludge reduction. In addition, metagenomics analysis uncovered that AOA bioreactors exhibited higher proportions of genes encoding enzymes involved in the glycolysis and denitrification processes, which contributed to the utilization of carbon sources as well as nitrogen consumption and thus sludge reduction. In spite of the economic benefits, this approach would help in lessening the waste sludge-related environmental issues.

Supplementary Materials: The following supporting information can be downloaded at: <https://www.mdpi.com/article/10.3390/membranes12070659/s1>, Figure S1: The temporal variations in basic quality parameters (DOC, TN, and TP) in effluents from MBRs (MBR_{control}, AOA₉₀, and AOA₈₀); Figure S2: The temporal variations of NO₃⁻-N and NH₄⁺-N in different tanks of MBR_{control}, AOA₉₀, and AOA₈₀; Figure S3: The MLSS concentration in different units of MBR_{control} (a), AOA₉₀ (b), and AOA₈₀ (c); Figure S4: The average polysaccharide and protein in SMP in different units of MBR_{control} (a and b), AOA₉₀ (c and d), and AOA₈₀ (e and f); Figure S5: EEM-PARAFAC components, tryptophan-like (C1), fulvic-like (C2), and humic-like (C3); Figure S6: The relative abundance of functional genes responsible for nitrogen metabolism in MBR_{control} (A), AOA₉₀ (B), and AOA₈₀ (C) (The subscript of A, B, and C means the sampling time). Table S1: Chemical composition of synthetic wastewater; Table S2: The average ± standard deviation of basic quality parameters of effluent in three different bioreactors (n = 25); Table S3: The average of NH₄⁺ and NO₃⁻ in the supernatant of different treatment units of MBRs (n = 14); Table S4: Sequencing of bacterial 16S rRNA gene along with alpha diversity of microbial taxa in three bioreactors.

Author Contributions: Conceptualization, Z.Z.; methodology, C.L., T.M. and H.K.; software, C.L. and T.M.; validation, Z.Z.; formal analysis, C.L.; investigation, C.L., T.M. and H.K.; resources, Z.Z.; data curation, Z.Z.; writing—original draft preparation, C.L. and T.M.; writing—review and editing, Z.Z.; visualization, C.L. and T.M.; supervision, Z.Z.; project administration, Z.Z.; funding acquisition, Z.Z. All authors have read and agreed to the published version of the manuscript.

Funding: This research was supported by the National Natural Science Foundation of China (52170041, 52050410336), Tsinghua SIGS Start-up Funding (QD2020002N), and the Committee of Science and Technology Innovation of Shenzhen (JCYJ20190813163401660).

Institutional Review Board Statement: Not applicable.

Informed Consent Statement: Not applicable.

Data Availability Statement: All data are available in the main text or Supplementary Materials.

Conflicts of Interest: The authors declare no conflict of interest.

References

1. Wang, Q.; Wei, W.; Gong, Y.; Yu, Q.; Li, Q.; Sun, J.; Yuan, Z. Technologies for reducing sludge production in wastewater treatment plants: State of the art. *Sci. Total Environ.* **2017**, *587*, 510–521. [CrossRef] [PubMed]
2. Zhou, H.; Li, X.; Xu, G.; Yu, H. Overview of strategies for enhanced treatment of municipal/domestic wastewater at low temperature. *Sci. Total Environ.* **2018**, *643*, 225–237. [CrossRef] [PubMed]
3. Liu, W.; Li, J.; Peng, Y. Impact of starvation conditions on the nitrifying performance and sludge properties in SBR system with a limited filamentous bulking state. *Sci. Total Environ.* **2021**, *797*, 148997. [CrossRef]
4. Cheng, C.; Geng, J.; Hu, H.; Shi, Y.; Gao, R.; Wang, X.; Ren, H. In-situ sludge reduction performance and mechanism in an anoxic/aerobic process coupled with alternating aerobic/anaerobic side-stream reactor. *Sci. Total Environ.* **2021**, *777*, 145856. [CrossRef] [PubMed]
5. Li, T.; Fan, Y.; Li, H.; Ren, Z.; Kou, L.; Guo, X.; Jia, H.; Wang, T.; Zhu, L. Excess sludge disintegration by discharge plasma oxidation: Efficiency and underlying mechanisms. *Sci. Total Environ.* **2021**, *774*, 145127. [CrossRef] [PubMed]

6. Ding, A.; Lin, W.; Chen, R.L.; Ngo, H.H.; Zhang, R.R.; He, X.; Nan, J.; Li, G.B.; Ma, J. Improvement of sludge dewaterability by energy uncoupling combined with chemical re-flocculation: Reconstruction of floc, distribution of extracellular polymeric substances, and structure change of proteins. *Sci. Total Environ.* **2022**, *816*, 151646. [[CrossRef](#)]
7. Feng, L.; Luo, J.; Chen, Y. Dilemma of Sewage Sludge Treatment and Disposal in China. *Environ. Sci. Technol.* **2015**, *49*, 4781–4782. [[CrossRef](#)]
8. Guo, W.-Q.; Yang, S.-S.; Xiang, W.-S.; Wang, X.-J.; Ren, N.-Q. Minimization of excess sludge production by in-situ activated sludge treatment processes—A comprehensive review. *Biotechnol. Adv.* **2013**, *31*, 1386–1396. [[CrossRef](#)]
9. Semblante, G.U.; Hai, F.I.; Ngo, H.H.; Guo, W.; You, S.-J.; Price, W.E.; Nghiem, L.D. Sludge cycling between aerobic, anoxic and anaerobic regimes to reduce sludge production during wastewater treatment: Performance, mechanisms, and implications. *Bioresour. Technol.* **2014**, *155*, 395–409. [[CrossRef](#)]
10. Pang, H.; Zhou, Z.; Niu, T.; Jiang, L.-M.; Chen, G.; Xu, B.; Jiang, L.; Qiu, Z. Sludge reduction and microbial structures of aerobic, micro-aerobic and anaerobic side-stream reactor coupled membrane bioreactors. *Bioresour. Technol.* **2018**, *268*, 36–44. [[CrossRef](#)]
11. Wang, K.; Zhou, Z.; Zheng, Y.; Jiang, J.; Huang, J.; Qiang, J.; An, Y.; Jiang, L.; Jiang, L.-M.; Wang, Z. Understanding mechanisms of sludge in situ reduction in anaerobic side-stream reactor coupled membrane bioreactors packed with carriers at different filling fractions. *Bioresour. Technol.* **2020**, *316*, 123925. [[CrossRef](#)] [[PubMed](#)]
12. Ferrentino, R.; Langone, M.; Gandolfi, I.; Bertolini, V.; Franzetti, A.; Andreottola, G. Shift in microbial community structure of anaerobic side-stream reactor in response to changes to anaerobic solid retention time and sludge interchange ratio. *Bioresour. Technol.* **2016**, *221*, 588. [[CrossRef](#)] [[PubMed](#)]
13. Niu, T.; Zhou, Z.; Shen, X.; Qiao, W.; Jiang, L.-M.; Pan, W.; Zhou, J. Effects of dissolved oxygen on performance and microbial community structure in a micro-aerobic hydrolysis sludge in situ reduction process. *Water Res.* **2016**, *90*, 369–377. [[CrossRef](#)] [[PubMed](#)]
14. Guo, J.-S.; Fang, F.; Yan, P.; Chen, Y.-P. Sludge reduction based on microbial metabolism for sustainable wastewater treatment. *Bioresour. Technol.* **2020**, *297*, 122506. [[CrossRef](#)]
15. Zhou, Z.; Zheng, Y.; Huang, J.; Jiang, L.M.; Jiang, J. Sludge reduction and microbial structures in MBRs: Features influencing the sustainable adoption of MBRs. In *Current Developments in Biotechnology and Bioengineering*; Elsevier: Amsterdam, The Netherlands, 2020. [[CrossRef](#)]
16. Zhao, X.; Jiang, J.; Zhou, Z. Responses of microbial structures, functions and metabolic pathways for nitrogen removal to different hydraulic retention times in anoxic side-stream reactor coupled membrane bioreactors. *Bioresour. Technol.* **2021**, *329*, 124903. [[CrossRef](#)]
17. Xiao, K.; Chen, Y.; Jiang, X.; Yang, Q.; Seow, W.Y.; Zhu, W.; Zhou, Y. Variations in physical, chemical and biological properties in relation to sludge dewaterability under Fe (II)—Oxone conditioning. *Water Res.* **2017**, *109*, 13–23. [[CrossRef](#)]
18. Lowry, O.; Rosebrough, N.; Farr, L.; Randall, R. Protein Measurement with the folin phenol reagent. *Enzyme Microb. Technol.* **1951**, *1*, 265–275. [[CrossRef](#)]
19. DuBois, M.; Gilles, K.A.; Hamilton, J.K.; Rebers, P.A.; Smith, F. Colorimetric Method for Determination of Sugars and Related Substances. *Anal. Chem.* **1956**, *28*, 350–356. [[CrossRef](#)]
20. Apha, A. *Standard Methods for the Examination of Water and Wastewater*; American Public Health Association: Washington, DC, USA; American Water Works Association: Washington, DC, USA; Water Environment Federation: Washington, DC, USA, 2005; Volume 21, pp. 258–259.
21. Lawaetz, A.J.; Stedmon, C.A. Fluorescence Intensity Calibration Using the Raman Scatter Peak of Water. *Appl. Spectrosc.* **2009**, *63*, 936–940. [[CrossRef](#)]
22. Maqbool, T.; Li, C.; Qin, Y.; Zhang, J.; Asif, M.B.; Zhang, Z. A year-long cyclic pattern of dissolved organic matter in the tap water of a metropolitan city revealed by fluorescence spectroscopy. *Sci. Total Environ.* **2021**, *77*, 144850. [[CrossRef](#)]
23. Ren, B.; Li, C.; Zhang, X.; Zhang, Z. Fe(II)-dosed ceramic membrane bioreactor for wastewater treatment: Nutrient removal, microbial community and membrane fouling analysis. *Sci. Total Environ.* **2019**, *664*, 116–126. [[CrossRef](#)] [[PubMed](#)]
24. Li, W.-W.; Sheng, G.-P.; Zeng, R.J.; Liu, X.-W.; Yu, H.-Q. China's wastewater discharge standards in urbanization. *Environ. Sci. Pollut. Res.* **2012**, *19*, 1422–1431. [[CrossRef](#)] [[PubMed](#)]
25. Huang, Z.; Ong, S.L.; Ng, H.Y. Performance of submerged anaerobic membrane bioreactor at different SRTs for domestic wastewater treatment. *J. Biotechnol.* **2013**, *164*, 82–90. [[CrossRef](#)] [[PubMed](#)]
26. Huang, J.; Wu, X.; Cai, D.; Chen, G.; Li, D.; Yu, Y.; Petrik, L.F.; Liu, G. Linking solids retention time to the composition, structure, and hydraulic resistance of biofilms developed on support materials in dynamic membrane bioreactors. *J. Memb. Sci.* **2019**, *581*, 158–167. [[CrossRef](#)]
27. Zhou, Z.; Qiao, W.; Xing, C.; Wang, C.; Jiang, L.-M.; Gu, Y.; Wang, L. Characterization of dissolved organic matter in the anoxic–oxic–settling–anaerobic sludge reduction process. *Chem. Eng. J.* **2015**, *259*, 357–363. [[CrossRef](#)]
28. Huang, H.; Ekama, G.; Deng, Y.-F.; Chen, G.-H.; Wu, D. Identifying the mechanisms of sludge reduction in the sulfidogenic oxic–settling anaerobic (SOSA) process: Side-stream sulfidogenesis-intensified sludge decay and mainstream extended aeration. *Water Res.* **2021**, *189*, 116608. [[CrossRef](#)]
29. Shao, Y.; Liu, G.; Wang, Y.; Zhang, Y.; Wang, H.; Qi, L.; Xu, X.; Wang, J.; He, Y.; Li, Q.; et al. Sludge characteristics, system performance and microbial kinetics of ultra-short-SRT activated sludge processes. *Environ. Int.* **2020**, *143*, 105973. [[CrossRef](#)]

30. Zheng, Y.; Hu, Z.; Tu, X.; Wu, K.; Chen, G.; Chai, X.-S. In-situ determination of the observed yield coefficient of aerobic activated sludge by headspace gas chromatography. *J. Chromatogr. A* **2020**, *1610*, 460560. [[CrossRef](#)]
31. Chae, K.J.; Oh, S.E.; Lee, S.T.; Bae, J.W.; Kim, I.S. The optimum substrate to biomass ratio to reduce net biomass yields and inert compounds in biological leachate treatment under pure-oxygen conditions. *Bioprocess Eng.* **2000**, *23*, 235–243. [[CrossRef](#)]
32. Ramdani, A.; Dold, P.; Déleris, S.; Lamarre, D.; Gadbois, A.; Comeau, Y. Biodegradation of the endogenous residue of activated sludge. *Water Res.* **2010**, *44*, 2179–2188. [[CrossRef](#)]
33. Liu, G.; Wang, J. Modeling effects of DO and SRT on activated sludge decay and production. *Water Res.* **2015**, *80*, 169–178. [[CrossRef](#)] [[PubMed](#)]
34. Di Iaconi, C.; De Sanctis, M.; Altieri, V.G. Full-scale sludge reduction in the water line of municipal wastewater treatment plant. *J. Environ. Manag.* **2020**, *269*, 110714. [[CrossRef](#)] [[PubMed](#)]
35. Chen, G.; Wu, W.; Xu, J.; Wang, Z. An anaerobic dynamic membrane bioreactor for enhancing sludge digestion: Impact of solids retention time on digestion efficacy. *Bioresour. Technol.* **2021**, *329*, 124864. [[CrossRef](#)] [[PubMed](#)]
36. Yang, J.; Zhang, X.; Sun, Y.; Li, A.; Ma, F. Formation of soluble microbial products and their contribution as electron donors for denitrification. *Chem. Eng. J.* **2017**, *326*, 1159–1165. [[CrossRef](#)]
37. Li, D.; Yang, J.; Li, Y.; Zhang, J. Research on rapid cultivation of aerobic granular sludge (AGS) with different feast-famine strategies in continuous flow reactor and achieving high-level denitrification via utilization of soluble microbial product (SMP). *Sci. Total Environ.* **2021**, *786*, 147237. [[CrossRef](#)]
38. Maqbool, T.; Cho, J.; Hur, J. Changes in spectroscopic signatures in soluble microbial products of activated sludge under different osmotic stress conditions. *Bioresour. Technol.* **2018**, *255*, 29–38. [[CrossRef](#)]
39. Chen, W.; Westerhoff, P.; Leenheer, J.A.; Booksh, K. Fluorescence Excitation-Emission Matrix Regional Integration to Quantify Spectra for Dissolved Organic Matter. *Environ. Sci. Technol.* **2003**, *37*, 5701–5710. [[CrossRef](#)]
40. Yu, G.H.; He, P.J.; Shao, L.M. Novel insights into sludge dewaterability by fluorescence excitation-emission matrix combined with parallel factor analysis. *Water Res.* **2010**, *44*, 797–806. [[CrossRef](#)]
41. Murphy, K.R.; Hambly, A.; Singh, S.; Henderson, R.K.; Baker, A.; Stuetz, R.; Khan, S.J. Organic matter fluorescence in municipal water recycling schemes: Toward a unified PARAFAC model. *Environ. Sci. Technol.* **2011**, *45*, 2909–2916. [[CrossRef](#)]
42. Ishii, S.K.L.; Boyer, T.H. Behavior of reoccurring parafac components in fluorescent dissolved organic matter in natural and engineered systems: A critical review. *Environ. Sci. Technol.* **2012**, *46*, 2006–2017. [[CrossRef](#)]
43. Fan, X.; Liu, C.; Yu, X.; Wang, Y.; Song, J.; Xiao, X.; Meng, F.; Cai, Y.; Ji, W.; Xie, Y.; et al. Insight into binding characteristics of copper (II) with water-soluble organic matter emitted from biomass burning at various pH values using EEM-PARAFAC and two-dimensional correlation spectroscopy analysis. *Chemosphere* **2021**, *278*, 130439. [[CrossRef](#)] [[PubMed](#)]
44. Yang, X.; Li, D.; Yu, Z.; Meng, Y.; Zheng, X.; Zhao, S.; Meng, F. Biochemical characteristics and membrane fouling behaviors of soluble microbial products during the lifecycle of *Escherichia coli*. *Water Res.* **2021**, *192*, 116835. [[CrossRef](#)] [[PubMed](#)]
45. Pinta, É.; Pacheco-Forés, S.I.; Wallace, E.P.; Knudson, K.J. Provenancing wood used in the Norse Greenlandic settlements: A biogeochemical study using hydrogen, oxygen, and strontium isotopes. *J. Archaeol. Sci.* **2021**, *131*, 105407. [[CrossRef](#)]
46. Cheng, C.; Zhou, Z.; Pang, H.; Zheng, Y.; Chen, L.; Jiang, L.-M.; Zhao, X. Correlation of microbial community structure with pollutants removal, sludge reduction and sludge characteristics in micro-aerobic side-stream reactor coupled membrane bioreactors under different hydraulic retention times. *Bioresour. Technol.* **2018**, *260*, 177–185. [[CrossRef](#)]
47. Chen, Y.; Jiang, X.; Xiao, K.; Shen, N.; Zeng, R.J.; Zhou, Y. Enhanced volatile fatty acids (VFAs) production in a thermophilic fermenter with stepwise pH increase—Investigation on dissolved organic matter transformation and microbial community shift. *Water Res.* **2017**, *112*, 261–268. [[CrossRef](#)]
48. Zhao, L.J.; Su, C.Y.; Wang, A.L. Comparative study of oxic granular sludge with different carbon sources: Effluent nitrogen forms and microbial community. *J. Water Process Eng.* **2021**, *43*, 102211. [[CrossRef](#)]
49. Liu, C.; Li, H.; Zhang, Y.Y.; Si, D.; Chen, Q. Evolution of microbial community along with increasing solid concentration during high-solids anoxic digestion of sewage sludge. *Bioresour. Technol.* **2016**, *216*, 87–94. [[CrossRef](#)]
50. Wang, P.; Wang, H.; Qiu, Y.; Ren, L.; Jiang, B. Microbial characteristics in anoxic digestion process of food waste for methane production—A review. *Bioresour. Technol.* **2018**, *248*, 29–36. [[CrossRef](#)]
51. Gao, P.; Xu, W.; Sontag, P.; Li, X.; Xue, G.; Liu, T.; Sun, W. Correlating microbial community compositions with environmental factors in activated sludge from four full-scale municipal wastewater treatment plants in Shanghai, China. *Appl. Microbiol. Biotechnol.* **2016**, *100*, 4663–4673. [[CrossRef](#)]
52. Mwanza, E.P.; Westhuizen, W.; Boucher, C.E.; Charimba, G.; Hugo, C. Heterologous expression and characterisation of a keratinase produced by *Chryseobacterium carnipullorum*. *Protein Express. Purif.* **2021**, *186*, 105926. [[CrossRef](#)]
53. Cheng, C.; Zhou, Z.; Niu, T.; An, Y.; Shen, X.; Pan, W.; Chen, Z.; Liu, J. Effects of side-stream ratio on sludge reduction and microbial structures of anaerobic side-stream reactor coupled membrane bioreactors. *Bioresour. Technol.* **2017**, *234*, 380–388. [[CrossRef](#)] [[PubMed](#)]
54. Zheng, Y.; Cheng, C.; Zhou, Z. Insight into the roles of packing carriers and ultrasonication in anoxic side-stream reactor coupled membrane bioreactors: Sludge reduction performance and mechanism. *Water Res.* **2019**, *155*, 310–319. [[CrossRef](#)] [[PubMed](#)]
55. Ju, F.; Xia, Y.; Guo, F.; Wang, Z.P.; Zhang, T. Taxonomic relatedness shapes bacterial assembly in activated sludge of globally distributed wastewater treatment plants. *Environ. Micro.* **2014**, *16*, 2421–2432. [[CrossRef](#)] [[PubMed](#)]

56. Wang, M.Y.; An, Y.; Huang, J.; Sun, X.; Yang, A.; Zhou, Z. Elucidating the intensifying effect of introducing influent to an anoxic side-stream reactor on sludge reduction of the coupled membrane bioreactors. *Bioresour. Technol.* **2021**, *342*, 125931. [[CrossRef](#)]
57. Świątczak, P.; Cydzik-Kwiatkowska, A.; Zielińska, M. Treatment of the liquid phase of digestate from a biogas plant for water reuse. *Bioresour. Technol.* **2019**, *276*, 226–235. [[CrossRef](#)]
58. Deng, L.; Guo, W.; Ngo, S.; Wang, X.; Hu, Y. Application of a specific membrane fouling control enhancer in membrane bioreactor for real municipal wastewater treatment: Sludge characteristics and microbial community. *Bioresour. Technol.* **2020**, *312*, 123612. [[CrossRef](#)]
59. Cheng, C.; Geng, J.; Zhou, Z.; Yu, Q.; Gao, R.; Shi, Y.; Wang, L.; Ren, H. A novel anoxic/aerobic process coupled with micro-aerobic/anaerobic side-stream reactor filled with packing carriers for in-situ sludge reduction. *J. Clean. Prod.* **2021**, *311*, 127192. [[CrossRef](#)]
60. Shi, Y.; Liu, T.; Chen, S.; Quan, X. Accelerating anaerobic hydrolysis acidification of dairy wastewater in integrated floating-film and activated sludge (IFFAS) by using zero-valent iron (ZVI) composite carriers. *Biochem. Eng. J.* **2022**, *177*, 108226. [[CrossRef](#)]
61. Ling, Y.; Moreau, J.W. Bacterial predation limits microbial sulfate-reduction in a coastal acid sulfate soil (CASS) ecosystem. *Soil Biol. Bioch.* **2020**, *148*, 107930. [[CrossRef](#)]
62. Xu, Z.; Dai, X.; Chai, X. Effect of different carbon sources on denitrification performance, microbial community structure and denitrification genes. *Sci. Total Environ.* **2018**, *364*, 195–204. [[CrossRef](#)]
63. Zheng, Y.; Quan, X.; Zhuo, M.; Zhang, X.; Quan, Y. In-situ formation and self-immobilization of biogenic Fe oxides in anaerobic granular sludge for enhanced performance of acidogenesis and methanogenesis. *Sci. Total Environ.* **2021**, *787*, 147400. [[CrossRef](#)] [[PubMed](#)]
64. Maughan, R. Carbohydrate metabolism. *Surgery* **2009**, *27*, 6–10. [[CrossRef](#)]
65. Yang, Y.; Chen, Y.; Guo, F.; Liu, X.; Su, X.; He, Q. Metagenomic analysis of the biotoxicity of titanium dioxide nanoparticles to microbial nitrogen transformation in constructed wetlands. *J. Hazard. Mater.* **2020**, *384*, 121376. [[CrossRef](#)] [[PubMed](#)]
66. Zhou, Z.; Qiao, W.; Xing, C.; An, Y.; Shen, X.; Ren, W.; Jiang, L.-M.; Wang, L. Microbial community structure of anoxic-oxic-settling-anaerobic sludge reduction process revealed by 454-pyrosequencing. *Chem. Eng. J.* **2015**, *266*, 249–257. [[CrossRef](#)]
67. Emmanuel, S.A.; Sul, W.J.; Seong, H.J.; Rhee, C.; Koh, S.C. Metagenomic analysis of relationships between the denitrification process and carbon metabolism in a bioaugmented full-scale tannery wastewater treatment plant. *World J. Microbiol. Biotechnol.* **2019**, *149*, 35. [[CrossRef](#)]